Physicochem. Probl. Miner. Process., 62(7), 2026, 230976

http://www.journalssystem.com/ppmp

Physicochemical Problems of Mineral Processing

ISSN 1643-1049

Comparative characterization of stearic acid-coated and uncoated commercial ground and precipitated calcium carbonates (GCC/PCC)

Bahri Ersoy [1], Hakan Çiftçi [1], Orhan Ozdemir [2], Salah Aldeen Al-Salahi [1]

[1] Afyon Kocatepe University, Engineering Faculty, Mining Engineering Department, Afyonkarahisar, Türkiye

[2] Istanbul Technical University, Mines Faculty, Mineral Processing Engineering Department, 34469, Maslak, Istanbul, Türkiye

Corresponding author: bersoy@aku.edu.tr (Bahri Ersoy)

Abstract: In this study, a series of characterization analyses were performed on both uncoated commercial calcites and commercial calcites modified via hydrophobic coating with stearic acid (SA); the effect of the coating process on specific physical properties (particle size distribution [PSD], BET surface area, porosity, bulk (or free flowing) density, and moisture content) and surface properties (water contact angle [θ_{water}], surface free energy [SFE], and zeta potential [ZP]) was investigated in detail. The commercial calcites used in the studies are Ground $CaCO_3$, GCC, Nidascarb 70; SA-coated/modified GCC; M-GCC, Nidascarb 70T; Precipitated $CaCO_3$, PCC, adaCAL N1, and SA-coated PCC; M-PCC, adaCAL N1C. The results showed that the hydrophobic coating process reduced the particle size of both products (GCC and PCC), but this reduction was more pronounced in fine particles. At the same time, it decreased and disappeared in coarse particles. One of the most striking results concerned surface area: the coating process increased the surface area of GCC, thereby decreasing the surface area of PCC, owing to PCC's porous aggregate structure composed of nano-cubic/rhombohedral crystal grains. It was determined that the total pore volume of PCC decreased from 1.04 cm^3/g to 0.83 cm^3/g after the coating process. According to θ_{water} data, the hydrophobic character of M-GCC (128.9°) was found to be higher than that of M-PCC (94.3°). Hydrophobic coatings significantly alter not only the surface properties but also the physical properties of both natural (GCC) and synthetic (PCC) calcites.

Keywords: hydrophobic coating, calcite, particle size, surface area, bulk density, moisture, contact angle, surface energy, zeta potential

1. Introduction

The term 'filler' is defined in many different ways in the literature depending on its origin (natural/synthetic, inorganic/organic), properties (particle shape, particle size, surface area, etc.), and areas of application (plastics, paper, paint coatings, etc.) (Wypych 2000; Rohleder and Huwald 2001; Ulusoy 2023). However, in general terms, fillers can be defined as fine-sized solid materials that can alter the processability and final product properties of the material into which they are embedded, and/or reduce production costs.

Fillers are widely used in the production of various industrial products, primarily paper, plastics, paints and coatings, concrete, asphalt, and cosmetics (Naydowski et al., 2001; Ulusoy, 2023). The amount of filler material used in paper production ranges from 5% to 40%, depending on the type of paper produced (Naydowski et al., 2001). In the plastics/polymer industry, the amount of filler used in the production of thermoplastics [polyvinyl chloride, polyethylene, polypropylene, polyamide, etc.], thermosets [unsaturated polyester resin, polyurethane, phenolic resin, etc.], elastomers [natural rubber, butyl rubber, etc.], adhesives, and sealants varies between 2% and 80% (Naydowski et al., 2001; Saçak, 2005). The amount of filler used in paint coatings ranges from 10% to 70%, depending on the type of paint (Nadolski et al., 2001).

DOI: 10.37190/ppmp/230976

Among the numerous mineral fillers known, including calcite, talc, kaolin, silica, barite, and mica, calcite is undoubtedly the most common and widely used filler worldwide due to its abundant reserves and low cost. Calcite is used in the plastics and paint coatings industry in both natural (ground calcium carbonate, GCC) and synthetic (precipitated calcium carbonate, PCC) forms, coated or uncoated depending on the product type. In contrast, in the paper and pharmaceutical industries, it is used without a permanent coating.

The main properties of mineral fillers can be listed as follows: particle shape, fineness (particle size) and PSD, surface area, surface coating/modification process and surface energy, true and bulk density, chemical purity, hardness, thermal conductivity, and optical (whiteness, refractive index) properties (Wypych, 2000; Naydowski et al., 2001; Ulusoy, 2023). It is known that fillers have a greater or lesser effect on the processability of the material into which they are embedded (paper/polymer pulp, paint suspension, etc.) and the properties of the final product (strength, heat/light/chemical resistance, hardness, surface smoothness, color, opacity, gloss, etc.) (Gill and Scott 1987; Lam et al., 2009; Lin et al., 2011; Zhao et al., 2016; Ulusoy, 2023). Whether this effect is more or less significant, or positive or negative, depends on the physical/chemical/surface properties of the filler material mentioned above (Gill and Scott, 1987; Saçak, 2005; Zhang et al., 2025). Therefore, in the production of any material, it is necessary to know and continuously monitor at least some of the most important parameters of the filler to be used (such as particle size, particle shape, surface area, color, oil absorption, bulk density, moisture content, and coating efficiency if a coating is to be applied). On the other hand, problems such as product flow difficulties and silo clogging that arise during the transportation, storage in silos, unloading from silos, and packaging of such fine-sized powder products produced by ore processing (crushing-grinding-screening/classification) or special chemical production methods, and which cause both time and economic losses in production facilities, stem mainly from two main reasons: one is design issues in silo/packaging/transportation design, and the other is fluctuations/changes in the basic properties of the products in question (Shinohara and Takahashi, 2006; Ulusoy, 2023).

Surface modification or coating applied to mineral fillers plays a significant role in the interaction between mineral particles and plastic materials (Lu et al., 2005). The primary function of surfactant is to reduce the relatively high surface energy of filler material, bringing it closer to the surface energy of the matrix (i.e., the polymer paste), thereby ensuring better dispersion of the filler within the matrix and improving the properties of the final product (Lu et al., 2005). However, some studies indicate that the applied coating filler significantly affects not only surface properties (hydrophobicity/θ_{water}, SFE, ZP, etc.) but also other physical properties (particle size, surface area, bulk density, moisture content, etc.) (Çayırlı et al., 2020; Huang et al., 2025). On the other hand, it is interesting to note that when examining the Technical Data Sheets (TDS) of commercial coated or uncoated PCC products with rhombohedral or cubic crystal structures, the primary crystal grain size determined by SEM or other specialized methods is generally reported. However, it is noteworthy that particle-size data (d_{10}, d_{50}, d_{90}), measured using widely applied methods such as laser diffraction and Sedigraph, are generally not included in the TDSs.

Another notable point is that both the effectively used uncoated GCC (Nidascarb 70) and the coated M-GCC (Nidascarb 70T) products in this study have the same particle size data in their TDS. Although there are numerous articles in the literature regarding the effect of coating on the surface properties (θ_w, ZP, etc.) of GCC/PCC, the number of studies investigating its effect on other physical properties (particle size, surface area, moisture content, etc.) is limited (Çayırlı et al., 2020; Huang et al., 2025). Çayırlı et al. (2020) found that the d_{50} of uncoated GCC, 5.2 µm, decreased to 4 µm after coating with 1% SA. Huang et al. (2025) investigated the hydrophobicity, water vapor adsorption, and other physical properties (particle size, surface area, porosity) of PCC with a constant coating ratio (4.2%) in slurry form using two different coating agents (SA and sodium stearate). In conclusion, they showed that the primary crystal grain size of PCC increased from 50 nm to 55-60 nm as seen in SEM and TEM images, but the average particle size (d_{50}) measured by laser diffraction decreased from 1.16 µm to 0.85-0.95 µm, and also that water vapor adsorption occurred as follows: Stearate-coated PCC > SA-coated PCC. Furthermore, it was determined that the BET surface area of uncoated PCC, 22.14 m^2/g, decreased to 21.96 m^2/g after coating with sodium stearate and to 18.82 m^2/g after coating with SA. It was also reported that the PCC coating pore volume decreased significantly.

Despite extensive research on stearic acid-coated calcium carbonate, direct comparative studies between commercially available GCC and PCC products under industrially relevant conditions remain scarce. Moreover, the effects of hydrophobic coating on both the physical properties (PSD, BET surface area, porosity, bulk density, and moisture content) and surface properties (θ_{water}, SFE, and ZP) have not been systematically evaluated within a unified experimental framework. In particular, the effect of stearic acid coating on commercially available PCC products with porous aggregate structures remains poorly understood.

Therefore, the objective of this study was to comparatively investigate the effects of stearic acid coating on the physical and surface properties of commercial GCC and PCC products. Coated (M-GCC and M-PCC) and uncoated (GCC and PCC) samples were characterized in terms of particle size distribution, morphology, BET surface area, porosity, bulk density, moisture content, θ_{water}, SFE, and ZP. The results provide a comprehensive comparison of the coating responses of natural and synthetic calcium carbonate products and contribute to a better understanding of the relationship among particle morphology, porosity, and surface-modification behavior.

2. Materials and methods

2.1. Materials

Commercial calcite powder products, both coated and uncoated with stearic acid (SA), were obtained from different companies. Information regarding the products used in this study is presented in Table 1. Particular attention was given to selecting commercial products with relatively fine particle sizes and comparable coating characteristics.

Table 1. Information on commercial powdered calcite products and their manufacturers used in this study

Commercial Product Name	Abbreviation	Description	Manufacturer Name (Place of Manufacture)
Nidaşcarb 70	GCC	Uncoated natural calcite	Nidaş Mining Industry and Trade Inc. (Nigde-Türkiye)
Nidaşcarb 70T	M-GCC	1% SA* coated natural calcite	
adaCAL N1	PCC	Synthetic calcite (Precipitated calcite)	Adaçal Industrial Minerals Inc. (Emirdag /Afyon/Türkiye)
adaCAL N1-C	M-PCC	3.9% SA* coated synthetic calcite	

GCC: Ground Calcium Carbonate; PCC: Precipitated Calcium Carbonate, M: Modified/Coated; *Declaration of companies

Chemical compositions of the samples were determined using a Rigaku Supermini X-ray fluorescence (WDXRF) spectrometer. As shown in Table 2, although the chemical compositions of both products are similar, the SiO_2 and Al_2O_3 contents in GCC and M-GCCC are higher than those in PCC and M-PCC.

Table 2. Chemical analyses of the products

Content (%)	GCC	M-GCC	PCC	M-PCC
CaO	53.90	55.20	54.20	54.52
SiO_2	1.00	0.44	0.08	0.16
Al_2O_3	1.03	0.19	0.02	0.05
MgO	0.08	0.33	0.08	0.21
SO_3	0.03	0.02	0.14	0.16
P_2O_5	0.06	0.05	0.11	0.01
Fe_2O_3	0.02	0.04	0.03	0.08
K_2O	0.03	0.04	0.02	0.03
SrO	0.03	0.03	0.03	0.03
LOI*	43.84	43.70	45.30	44.76

*Loss on ignition

2.2. Methods

2.2.1. FTIR analysis

FTIR analyses of calcite products and SA were performed using the FTIR instrument (Thermo Scientific™ Nicolet™ IS5 FTIR Spectrometer) located in the Polymer Chemistry Laboratory of the Department of Chemistry. FTIR spectra were recorded over the range 400–4000 cm^{-1} at a resolution of 4 cm^{-1} using the KBr pellet technique. The KBr pellets were prepared by mixing the calcite sample with KBr powder (around 1:100) and using a hydraulic press.

2.2.2. Particle size distribution (PSD) analysis

Particle size distribution (PSD) analysis of powdered calcite samples was performed using the wet method with a Malvern Mastersizer 2000/Hydro 2000MU instrument, which analyzes based on the principle of laser diffraction. In the measurements, while pure water was used for uncoated products (GCC and PCC), isopropyl alcohol (2-propanol) was used as the dispersing medium for coated products (M-GCC and M-PCC). Approximately 0.01 g of the sample was added to a 1-liter beaker containing 800 mL of pure water (or isopropyl alcohol), and the "laser obscuration" value was maintained within the green range (3-10%). The mixture was stirred for 1 min, followed by 1 min of ultrasonic vibration, after which particle-size measurements were performed. The device performs three separate measurements for each sample during analysis and provides the average of these three measurements as a final result. The pure water used during the measurements had a conductivity of 3.4 µS/cm and a pH value of approximately 7.4.

2.2.3. SEM analysis

SEM analyses were performed to examine the particle morphology of coated (M-GCC and M-PCC) and uncoated (GCC and PCC) calcites and to verify the particle-size analysis results obtained by the laser diffraction method described above. These analyses were performed using SEM instruments at AKU-TUAM (Zeiss EVO 50) and Adaçal (Zeiss EVO LS10), and the powder samples were coated with gold using a coating device prior to measurement.

2.2.4. BET surface area measurement

BET surface areas (m^2/g) of the powder samples were measured using a BET device (Quantachrome Instruments-NOVA 2200e), and the samples were degassed at 200 °C for 2 hours before measurement.

2.2.5. Porosity analysis with a mercury porosimeter

Porosity analyses of PCC and M-PCC products were performed using a mercury porosimeter (Anton Paar Quantachrome Poremaster 60) in the Central Research Laboratory of RTE University. Pore size distribution and cumulative pore volume curves as a function of pore diameter were obtained. Approximately 0.60 g of sample was used in the measurement.

2.2.6. Contact angle (θ) measurement and determining the OWRK-Fowkes SFE

Before contact angle (θ) measurements, calcite powder samples were compressed into tablets (32 mm in diameter) using a hydraulic press at 300 bar pressure. Next, these prepared tablets were placed in the contact angle measuring device (KSV Attension ThetaLite TL 101-Biolin Scientific), the camera settings were adjusted, a drop of liquid was placed on them, and θ was measured immediately. Two types of liquids were used in the measurements: one polar (water) and one non-polar (bromonaphthalene). The θ value measured at 2 sec served as the basis for interpretation and SFE energy calculations. Three different images (θ) were taken from different locations on each tablet sample, and the average or closest measurement was recorded as θ. While the water droplet volume was approximately 6-8 µL, the bromonaphthalene droplet volume was approximately 3-4 µL. Laboratory measurements recorded an ambient temperature of 25-27 °C and a humidity level of 32-34%. Before the θ measurement, an air-blowing process was applied to remove any potential dust particles from the tablet samples' surfaces, and no other special surface-cleaning process was performed. After the measurements, the θ values

obtained for each liquid were calculated using the instrument via two equations with two unknowns in the OWRK-Fowkes equation (Eq. 1) given below to determine the SFE (γ_s) of the calcite products and their polar ($\gamma_{sv}^{p} = \gamma_{s}^{p}$) and distributional ($\gamma_{sv}^{d} = \gamma_{s}^{d}$ components.

Here, γ_s is equal to the sum of the components γ_s^p ve γ_s^d.

$$\sqrt{\gamma_{sv}^{d}\gamma_{lv}^{d}} + \sqrt{\gamma_{sv}^{p}\gamma_{lv}^{p}} = 0{,}5\ \gamma_{lv}(1 + \cos\theta) \quad (1)$$

Additionally, to verify the reproducibility of the measurements, contact angle measurements were repeated on independently prepared tablets, and consistent results were obtained.

2.2.7. Zeta potential (ZP) measurements

ZP measurements of powder samples were performed using a zetameter (Malvern-Zetasizer Nano Series Nano-Z) in Adaçal. 100 mL of distilled water was added to a 250 mL beaker, placed on a magnetic stirrer, and a small amount (≈0.1 g) of sample was added using a spatula and stirred for 2 min. Then, a sample was taken from the suspension with a syringe and injected into the ZP measurement cell, taking care to avoid air gaps. The cell was then placed in its position on the zetameter, and first the conductivity, then the ZP measurement was performed. The measurement temperature on the zetameter was set to 20 °C. After stirring and before the ZP measurement, the suspension's natural pH was measured and recorded with a pH meter. The conductivity of the distilled water used was 3.4 µS/cm, and the pH value was ≈7.4. pH measurements were performed using a pH meter (Mettler Toledo SevenExcellence) with an accuracy of ±0.001.

2.2.8. Moisture analysis

The moisture content of the products was determined using a rapid IR (infrared) moisture analyzer (AND MX-50) at 105°C. Approximately 2.5 g of powder sample was used. The sensitivity of the device was ±0.01 (%). Three analyses were performed for each product, and the average value was taken.

2.2.9. Determination of bulk (or free flowing) density

The bulk densities of the products were determined using equipment manufactured in accordance with DIN ISO 697 (Haver & Boecker OHG). A sample of the product to be measured was taken and placed in the equipment's upper chamber. Then, the lower lid of the chamber was opened, and the sample was poured into a sample cell (500 mL volume and 605.4 g tare weight). The sample cell was then weighed to determine the product's bulk density. Three analyses were performed for each product, and the average value was taken.

3. Results and discussion

3.1. FTIR analysis

To observe the interactions of the coating agent SA with GCC and PCC, FTIR spectra of SA were obtained along with uncoated (GCC and PCC) and coated powdered calcite samples, and the resulting spectra are given in Fig. 1. The peaks of SA in the 2850-2950 cm^{-1} band arise from the characteristic C-H stretching vibration in the hydrocarbon chain of SA, while the peak in the 1700 cm^{-1} band originates from the characteristic C=O stretching vibration in the carboxyl (COOH) group of SA, the peaks in the 1300-1500 cm^{-1} band originate from the C-H bending vibration of the hydrocarbon chain, and the peaks in the 700-950 cm^{-1} band, referred to in the literature as the fingerprint region (1300-650 cm^{-1}), originate from the C-O bending vibration in the carboxyl group (Yıldız et al., 1997; Stuart et al., 1998; Croitoru et al., 2017). As described in the literature (Salisbury et al., 1991; Shi et al., 2010; Croitoru et al., 2017), characteristic calcite peaks are observed in the FTIR spectra of both uncoated GCC and PCC, as well as coated M-GCC and M-PCC. The strongest of these peaks is observed at approximately 1440 cm^{-1} and originates from the C-O asymmetric stretching vibration in the CO_3 group. Other strong peaks observed in the range of 712 cm^{-1} to 874 cm^{-1} correspond to C-O bending vibrations in the CO_3 group. The peak observed at 1797 cm^{-1} is assigned to the C-O symmetric stretching vibration (Rodriguez-Blenco, 2011). Comparing the spectra of GCC and PCC with those of M-GCC and M-PCC reveals two small peaks in

the 2850-2950 cm^{-1} band in the coated/modified products. These peaks are characteristic C-H stretching vibrations in the hydrocarbon chain of SA and indicate that hydrophobic coating occurred. However, notably, these peaks in the M-PCC are somewhat stronger and sharper than those in the M-GCC.

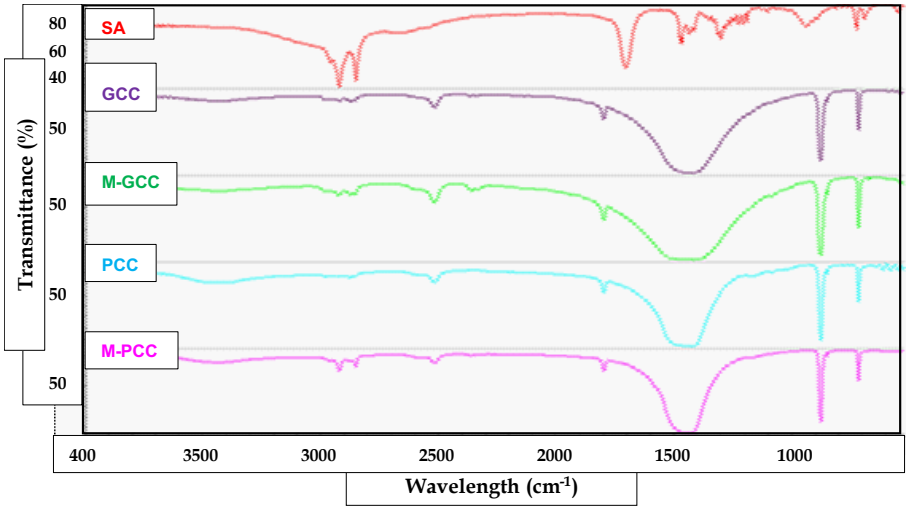

Fig. 1. FTIR spectra of uncoated (GCC and PCC) and coated (M-GCC and M-PCC) powdered calcite products and stearic acid (SA) used in the coating

3.2. Particle size distribution (PSD) and SEM analyses

Normal distribution curves obtained from the PSD analysis of coated and uncoated products are given in Fig. 2. Cumulative undersized (CUS) curves are given in Fig. 3. Evaluation of the PSD and CUS curves together indicates that the particle size distributions of the hydrophobically coated products shifted toward smaller particle sizes, suggesting an increase in the amount of fine-sized material. However, this leftward shift is more pronounced at finer sizes, while it decreases and disappears at larger sizes; in fact, a rightward shift, i.e., particle coarsening, is even observed for M-PCC. The reduction in particle sizes of GCC and PCC observed after coating may be attributed to the adsorption of SA molecules on the particle surfaces, which lowers surface energy and reduces particle agglomeration.

In the literature, this mechanism is known to play a particularly important role in the aggregation of colloidal- and nano-sized mineral particles (Lin et al., 2002; Teychené et al., 2020; Ersoy et al., 2026). However, this is not true for all particles in the product; in other words, the tendency to aggregate together persists despite the hydrophobic coating on larger particles. This behavior may indicate that the coating process affects fine and coarse particles differently. Specifically, with relatively fine particles, the coating process primarily disperses the particles by reducing surface energy, thereby decreasing the tendency for aggregation; with relatively large particles, hydrophobic attractive forces come into play, preventing dispersion.

In the literature, a study on the relationship between mineral particle size and hydrophobic force using modified nano-silica reported that increasing the particle size increased the hydrophobic attractive force (Zhang et al., 2024). The d_{10}, d_{50} (average), d_{90}, and d_{97} (top cut) values, which represent the fine, medium (i.e., average), coarse, and very coarse (top cut) portions of the products and are commonly used in practice, are given in the small table in Fig. 3. As seen in Fig. 3, the particle size of M-GCC is finer than that of GCC. However, this difference is more pronounced at d_{10} and d_{50}, but not so much at d_{90} and d_{97}. The average particle size (d_{50}) for GCC was 2.59 µm, and for M-GCC, 2.03 µm. A similar result was reported in a study on GCC modification (Çayırlı et al., 2020), which found that the SA coating process reduced the d_{50} particle size from 5.2 µm to 4 µm. However, the situation is different for PCC: while a decrease in d_{10} and d_{50} values is observed after coating, increases were observed in d_{90} and especially d_{97} values. The average particle size (d_{50}) for PCC was 8.49 µm, and for M-PCC, 6.82 µm.

In a study in the literature (Huang et al., 2025), PSD curves similar to those in this study were obtained using rhombohedral PCC, and it was determined that the coating process broadened the PSD curve and reduced the d_{50} particle size; however, no information was given for larger particle sizes such

as d_{90} and d_{97}. On the other hand, comparing the curves of natural calcite (GCC) and synthetic calcite (PCC) reveals a significant difference in particle size between the two, with GCC being finer than PCC. A similar situation exists between modified products (M-GCC and M-PCC). This is because the production processes for GCC and PCC are different.

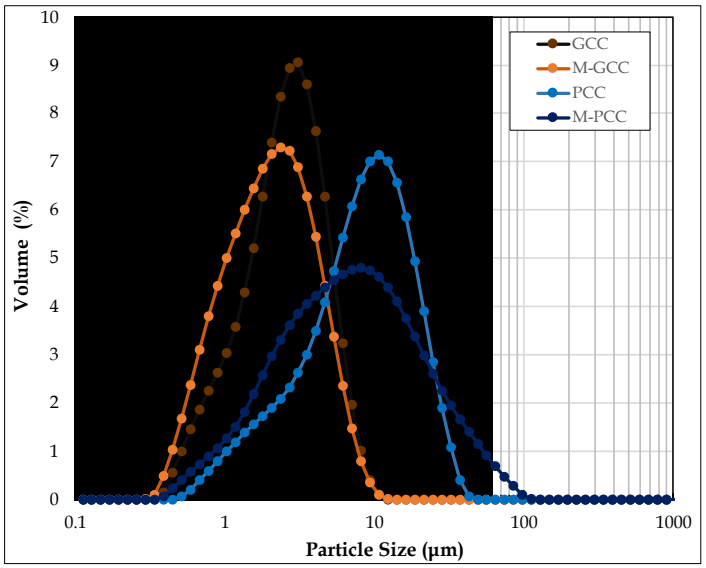

Fig. 2. Normal distribution curves of particle size of products measured in wet environment

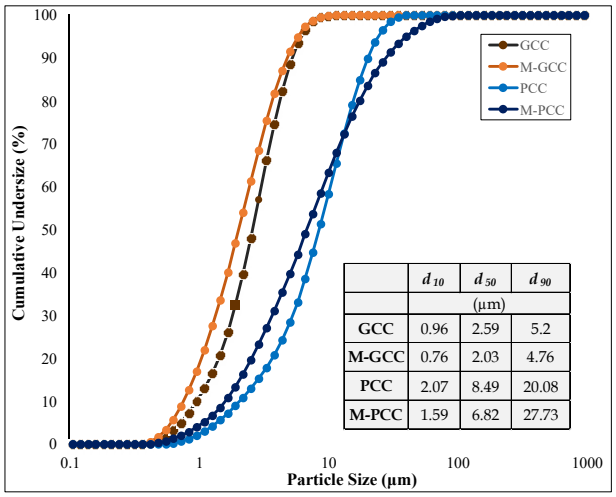

	d_{10}	d_{50}	d_{90}
	(µm)		
GCC	0.96	2.59	5.2
M-GCC	0.76	2.03	4.76
PCC	2.07	8.49	20.08
M-PCC	1.59	6.82	27.73

Fig. 3. Cumulative particle size curves and d_{10}-d_{97} table data of products measured in wet environment

GCC is a natural product produced by grinding naturally occurring calcite ($CaCO_3$), while PCC is a synthetic product produced by chemical precipitation in a reactor. GCCs generally consist of irregular, angular, blocky, non-porous particles (Figs. 4a and b). In contrast, PCC particles are spherical or irregular aggregates and contain porosity due to the aggregation of nano-sized cubic/rhombohedral primary crystals formed during reactor fabrication (Figs. 5a and b, Figs. 6 and 7).

SEM analyses were performed to examine the particle morphologies of the products and to validate the PSD data measured by laser diffraction. As shown in the SEM images the SEM in Figs. 4a, b and 5a, b, the coated products exhibit a slightly smaller average particle size (d_{50}) than their uncoated counterparts, and these images support the PSD analysis results.

3.3. BET surface area measurement and porosity analysis

BET surface area measurements for coated and uncoated products are presented in Table 3. As shown in Table 3, the surface areas of both the coated (M-PCC) and uncoated (PCC) synthetic calcites are significantly higher than those of natural calcites (GCC/M-GCC). The main reason for this is that natural

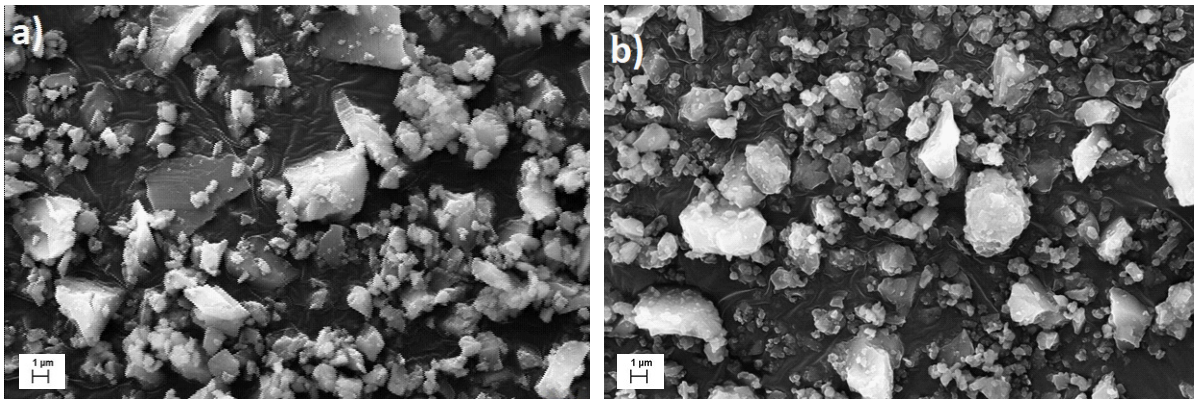

Fig. 4. SEM images of GCC (a) and M-GCC (b) products taken at 7000X magnification

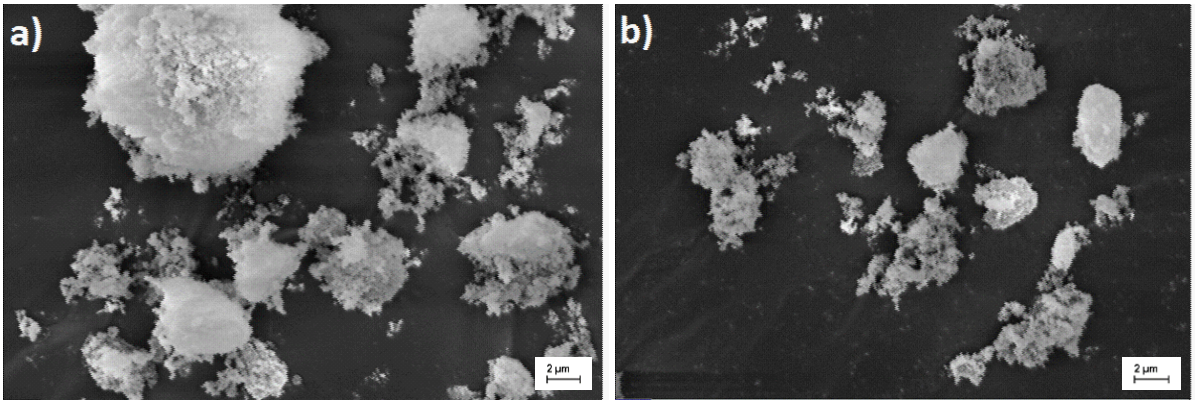

Fig. 5. SEM images of PCC (a) and M-PCC (b) products taken at 7000X magnification

significantly higher than those of natural calcites (GCC/M-GCC). The main reason for this is that natural calcites exist as non-porous solid masses (Figs. 4a and b). In contrast, synthetic calcites consist of nanosized crystalline grains and contain porosity (Figs. 6 and 7). As seen in the SEM images given in Figs. 6a and 6b, PCC and M-PCC aggregates/particles, consisting of primary cubic/rhombohedral crystal grains, generally exhibit porosity.

As shown in Figs. 7a and 7b, approximately 90% of the pore volume in PCC and 75% in M-PCC corresponds to macropores (>50 nm), while the remaining pore volume consists of micropores (2-50 nm). According to the mercury porosimeter analysis, the total pore volumes of PCC and M-PCC are 1.04 and 0.83 cm^3/g, respectively, with a slight decrease in pore volume after coating. On the other hand, the coating process caused a significant decrease in the surface area of PCC (from 30.03 m^2/g to 19.79 m^2/g), while it caused the opposite increase in GCC (from 4.28 m^2/g to 5.54 m^2/g) (Table 3).

Table 3. BET surface areas and average particle sizes of powdered calcite products

Products	BET Surface Area (m^2/g)	d_{50} Particle Size (µm)
GCC	4.28	2.59
M-GCC	5.54	2.03
PCC	30.03	8.49
M-PCC	19.79	6.82

The decrease in surface area of PCC after the coating process may have resulted from these two reasons: Firstly, SA molecules entering the pores during coating narrow the pore diameters and reduce the total pore volume. As shown in Fig. 7a, the pore size distribution curve exhibits a slight shift toward smaller pore diameters after coating. Secondly, surface irregularities and/or particle boundaries in PCCs are partially masked by the adsorption of SA molecules onto particle surfaces. The likely reason

for the increase in GCC surface area after coating is that the decrease in surface energy prevents aggregation of colloidal-sized (<1 μm) particles within the product, thereby increasing the number of free particles. The decrease in the GCC d_{50} value presented in Table 3 supports this interpretation. Similar results have been obtained in studies in the literature that investigated the effects of SA modification of PCC (Huang et al. 2025) and GCC (Çayırlı et al. 2020) on particle size and surface area.

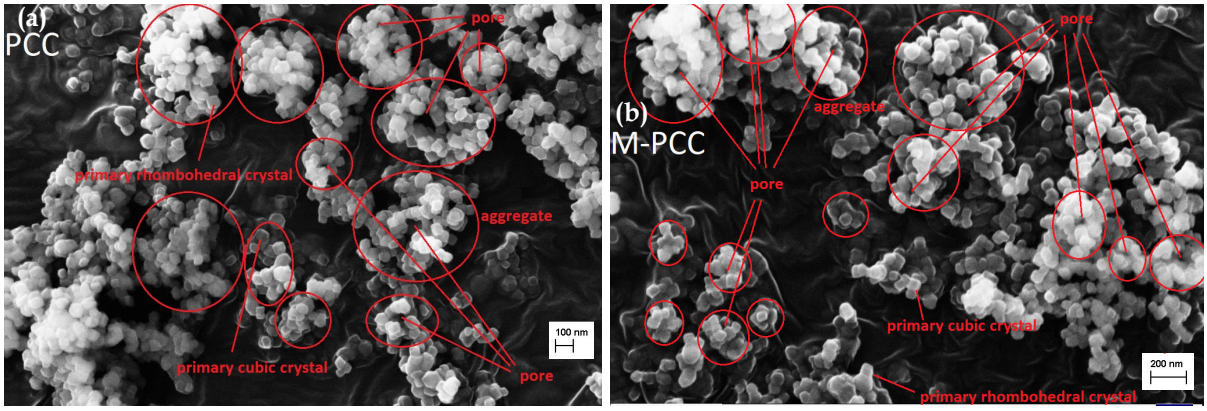

Fig. 6. SEM images of PCC (a) and M-PCC (b) particles/aggregates containing porosity and consisting of primary cubic/rhombohedral crystal grains (Magnification: 80000X)

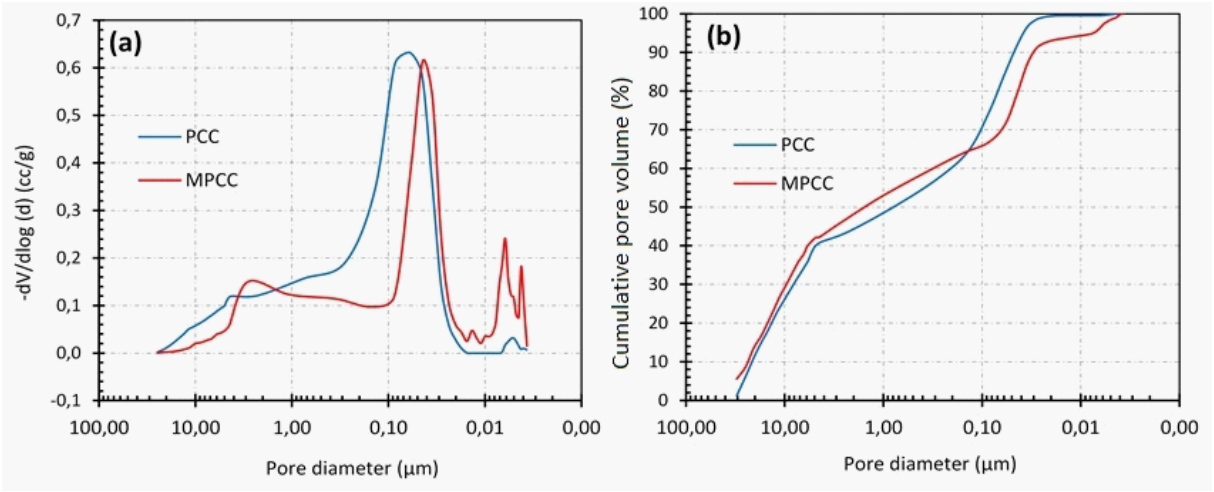

Fig. 7. Pore size distribution (a) and cumulative pore volume (b) curves of PCC and M-PCC as a function of pore size

3.4. Moisture and bulk (or free flowing) density analyses

The moisture content analysis results and bulk densities of the products are given in Table 4. As expected, the coated products (M-GCC and M-PCC) exhibited lower moisture contents than the uncoated products (GCC and PCC). However, this decline was more pronounced in PCC compared to GCC. After the coating process (M-GCC and M-PCC), the moisture content of GCC and PCC decreased to 0.22% and 0.34%, respectively.

This is because the coating agent SA, which adheres to the particle surfaces, makes the particles hydrophobic by reducing their attraction to water due to the hydrophobic HC chains on the particle surfaces. Notably, the reduction in moisture content was more pronounced for PCC than for GCC after coating (approximately 44%) and is much greater than the reduction in GCC (approximately 21%). On the other hand, the results indicate that coated or uncoated synthetic calcites (PCC and M-PCC) have higher moisture content than natural calcites (GCC and M-GCC). The main reason is that synthetic products have a higher BET surface area, which depends on their particle morphology.

Comparing the bulk density values in Table 4, synthetic calcites (PCC and M-PCC) have lower bulk

Table 4. Results of moisture and bulk density analysis of powdered calcite products

Products	Moisture (%)	Bulk Density (g/cm³)
GCC	0.28 ±0.01	0.60 ±0.02
M-GCC	0.22 ±0.02	0.73 ±0.03
PCC	0.62 ±0.03	0.38 ±0.01
M-PCC	0.34 ±0.02	0.41 ±0.01

densities than natural calcites (GCC and M-GCC). This is due to the porosity of synthetic calcites (PCC/M-PCC) (Figs. 6 and 7). Also, their relatively looser packing is due to their larger particle sizes (Fig. 3). When comparing the bulk densities of coated products (M-GCC and M-PCC) and uncoated products (GCC and PCC), it was observed that the bulk density increased after coating. Still, this increase was greater in GCC and less in PCC. The bulk densities of GCC and PCC are 0.60 and 0.38 g/cm³, respectively, while those of M-GCC and M-PCC are 0.73 and 0.41 g/cm³, respectively. The primary reason for the increase in bulk density after coating is the widening of the PSD range. As shown in Fig. 2, the curves of the coated products are shifted to the left, and the PSD range widens. This change and expansion occurred to a lesser extent for GCC and to a greater extent for PCC. The widening of the PSD range resulted in better packing and increased bulk density. This is a common/typical issue encountered in the literature (Suzuki 2006, Pal et al. 2014, Kleba-Ehrhardt et al. 2025) regarding the packaging of various powder products. Additionally, the lubricating effect of SA molecules adhering to particle surfaces contributed to close packing of the coated products. As is known, surfactants such as SA are among the most widely used and effective lubricants in practice (Reed, 1994).

3.5. Contact angle (θ) and surface free energy (SFE)

The primary aim of surface coating is to reduce the surface energy of GCC and PCC products, which naturally possess relatively high surface energy and hydrophilic properties, by making them hydrophobic. This will result in a more homogeneous/better dispersion within the medium (polymer paste, etc.). In this context, the hydrophobicity of coated and uncoated calcites was determined by measuring θ_{water} values, and the OWRK-Fowkes SFE values were also calculated using a contact angle measuring device with θ data for water and bromonaphthalene. The results obtained are given in Fig. 8, and the θ_{water} photographs are given in Fig. 9. As shown in Figs. 8 and 9, uncoated commercial products have θ_{water} values of zero or very low (PCC: 0°; GCC: 14.2°) and are extremely hydrophilic; after coating with SA, these values increase to 94.3° and 128.9°, respectively, indicating the development of hydrophobic surface characteristics.

Furthermore, the GCC modification process was superior to that of PCC, indicating that M-GCC was more hydrophobic than M-PCC. The difference in θ_{water} values between the M-PCC and M-GCC may be attributed to differences in coating processes, particle morphologies, and, consequently, specific surface areas. GCC is coated using the dry method, while PCC is coated using the wet method. Furthermore, according to information provided by the companies, the amount of SA used in the coating is 1% for GCC and 3.9% for PCC; surface area values measured with a BET device are 4.28 m²/g for GCC and 30 m²/g for PCC.

In the literature, when θ_{water} measurements were performed on PCC samples coated with different surfactants such as SA and combined DDP (dodecyl dihydrogen phosphate), similar results were obtained, albeit with minor differences. In a study by Barhoum et al. (2014), it was determined that the θ_{water} value of PCC synthesized with scalenohedral morphology was 25°, but when an anionic surfactant (sodium oleate) was added to the reactor during synthesis, the crystal morphology of PCC changed to rhombohedral, and the θ_{water} value increased to 130°. In the study by Zhao et al. (2016), the θ_{water} value of PCC increased from 0° to 119° upon modification with 2% DDP. Atta et al. (2016) measured the θ_{water} values of PCCs modified with different fatty acids [steric acid (SA), oleic acid (OA), linoleic acid (LOA), and epoxidized oleic acid [EOA)] at superhydrophobic levels (150°-153°). In another study by Ghosh et al. (2012), the θ_{water} value of GCC was measured at ≈ 0°, whereas that of GCC modified with PMMS (polymethylphenyl methoxy siloxane) was 142°. In another study on SA-coated and uncoated natural

calcite (Uçurum and Özdemir 2024), the θ_{water} values for GCC and M-GCC were determined to be 13.52° and 101.66°, respectively.

The value for GCC is close to our study's result, but the value for M-GCC is lower. The differences between the θ_{water} values observed in the literature and the values measured in this study, especially for hydrophobic coated calcite (M-GCC or M-PCC), are generally due to differences in experimental conditions [type of surfactant used in coating, surfactant dosage, coating time, coating method, etc.] and/or physical properties (particle shape/morphology, particle size, surface area, etc.) of the calcite samples used. According to the SFE results shown in Fig. 8, the GCC and PCC SFE values are 76-78 mJ/m² and decrease to 38-39 mJ/m² after coating. According to the SFE data obtained from the contact angle measuring device, the polar components (γ_{SV}^{p}) of GCC and PCC SFEs constitute approximately 43-44% of the total SFE, while this rate decreases to 1.5-10% in coated products (M-GCC and M-PCC). This is due to SA, a surfactant with a hydrophobic HC chain adsorbed onto the calcite surface.

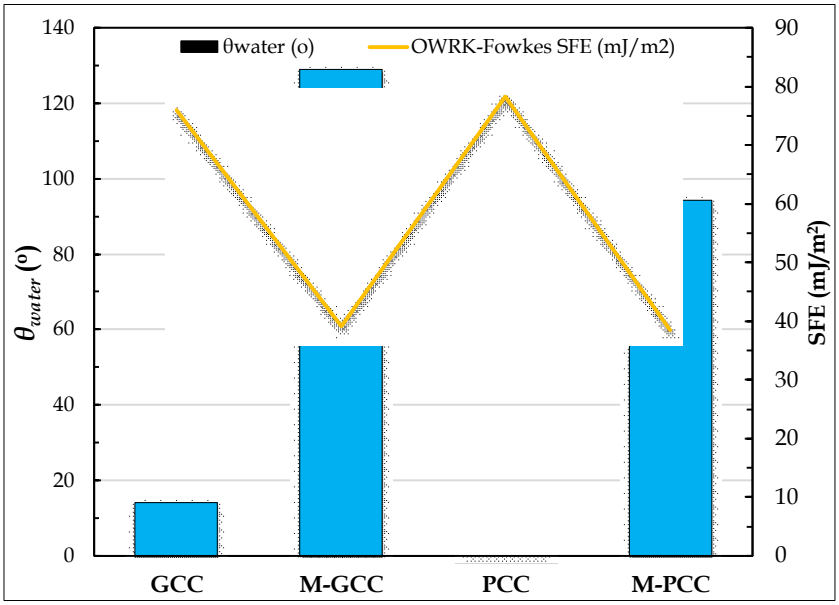

Fig. 8. Measured water contact angles (θ_{water}) of coated (M-GCC and M-PCC) and uncoated (GCC and PCC) calcite tablets and the calculated OWRK-Fowkes SFE values obtained from them

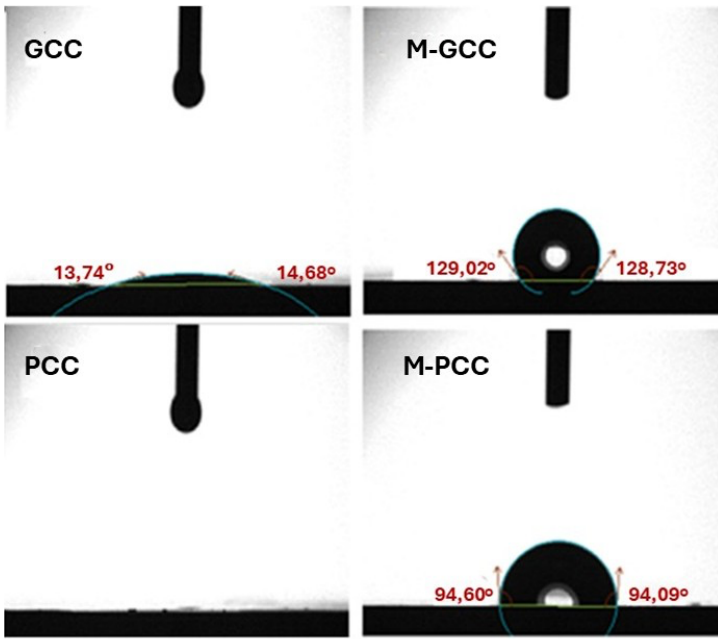

Fig. 9. Photographic images of the θ_{water} on coated (M-GCC and M-PCC) and uncoated (GCC and PCC) calcite tablets

3.6. Zeta potential (ZP) measurements

ZP data, suspension pH, and conductivity (µS/cm) values of the products, recorded in their natural state immediately before measurement (i.e., without the use of any pH regulator), are given in Fig. 10. The zeta potential values of GCC and PCC were positive under natural suspension (GCC +19.6 mV; PCC +12.4 mV, respectively). Following the SA treatment, the zeta potentials became negative, indicating adsorption of SA molecules on the calcite surfaces. The measured zeta potentials were -9.5 mV for M-GCC and -14.4 mV for M-PCC. This is because the stearate anion, the anion component of the SA molecule, forms chemical bonds with the lattice cation Ca (>Ca^{2+}) that forms calcite, or with Ca^{2+} ions that dissolve in the medium and are subsequently adsorbed back onto the calcite surface; or, depending on the conditions (if the concentration of SA and Ca^{2+} in the medium is sufficiently high), these Ca^{2+} ions combine with stearate anions and precipitate as Ca-Stearate on the calcite surface (Song et al., 2003; Mihajlovich et al., 2013; Cao et al., 2016). Song et al. (2003) measured the ZP value of PCC at natural pH to be ≈ +15 mV and found that it shifted from positive to negative as the stearate ion concentration increased, reaching -10 mV. Their results appear to be consistent with the data obtained in this study. When comparing the ZPs of natural (M-GCC) and synthetic (M-PCC) calcites after coating, the ZP of M-PCC (-14.4 mV) is slightly higher in absolute terms than that of M-GCC (-9.5 mV). Therefore, it is expected that electrostatic and van der Waals (ion-dipole) interactions between cations and/or polar functional groups within the structures (polymer matrix, paint, etc.) are stronger in M-PCC than in M-GCC.

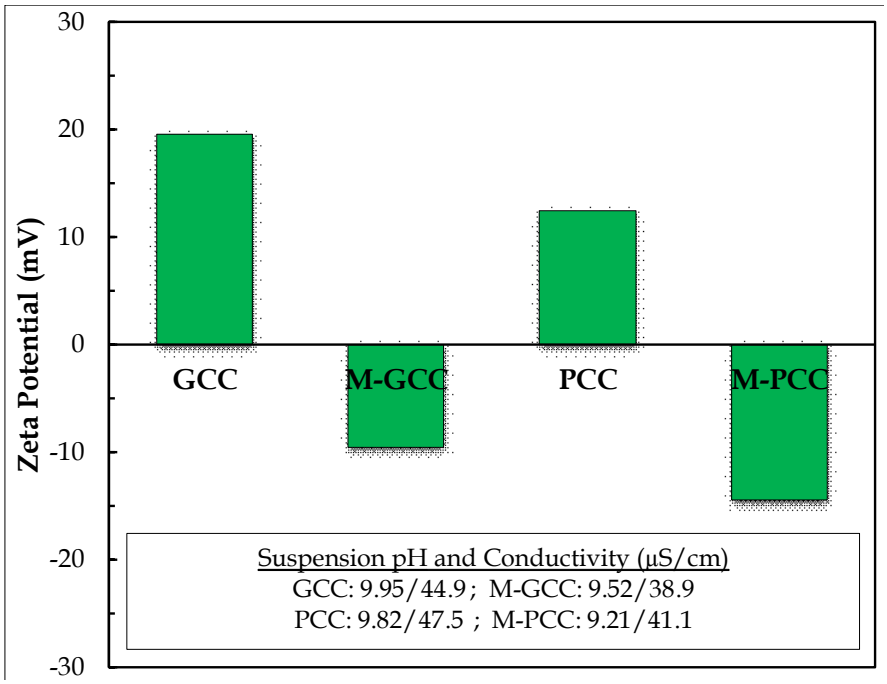

Fig. 10. Zeta potential (ZP) values, native pH values, and conductivity of coated (M-GCC and M-PCC) and uncoated (GCC and PCC) calcites

3.7. General discussion

The results obtained in this study are generally consistent with those reported in previous studies regarding the influence of stearic acid coating on calcium carbonate fillers. As summarized in Table 5, stearic acid coating consistently reduced the average particle size. It increased the hydrophobicity of both GCC and PCC, while converting the zeta potential from positive to negative. However, the response of BET surface area differed between GCC and PCC because of their fundamentally different particle morphologies and pore structures. Minor differences in the magnitude of the reported values among different studies are expected. They can be attributed to variations in raw material characteristics, crystal morphology, coating method (dry or wet), coating dosage, commercial production conditions, and characterization techniques. It should also be emphasized that the

commercial GCC and PCC products investigated in this study were manufactured using different industrial coating processes with different coating levels. Therefore, the effects of coating were evaluated only within each material pair (GCC vs. M-GCC and PCC vs. M-PCC). In contrast, comparisons between GCC-based and PCC-based products are presented solely to describe the characteristics of commercially available calcium carbonate fillers rather than to compare coating efficiencies.

Table 5. Comparison of the present results with representative literature

Property	Present study	Representative literature	Comparison	Possible explanation
Particle size (GCC) (μm)	d_{50}: 2.59 → 2.03	5.2 → 4.0 (Çayırlı et al., 2020)	Same trend	Reduced surface energy suppresses fine-particle agglomeration after coating.
Particle size (PCC) (μm)	d_{50}: 8.49 → 6.82	1.16 → 0.86–0.95 (Huang et al., 2025)	Same trend	Different commercial PCC grades, crystal morphology, and production conditions.
BET surface area (GCC) (m^2/g)	4.28 → 5.54	Increase after coating (Çayırlı et al., 2020)	Consistent	Dispersion of fine particles increases accessible surface area.
BET surface area (PCC) (m^2/g)	30.03 → 19.79	22.14 → 18.82 (Huang et al., 2025)	Excellent agreement	Partial pore filling by stearic acid and masking of pore surfaces reduce BET area.
Pore volume (PCC) (cm^3/g)	1.04 → 0.83	Decreased after coating (Huang et al., 2025)	Consistent	Partial pore filling by stearic acid molecules.
Water contact angle (GCC)	14.2° → 128.9°	13.5° → 101.7° (Uçurum & Özdemir, 2024): coated GCC ≈142° (Ghosh et al., 2012)	Same trend	Different coating conditions, particle size, morphology, and surface area.
Water contact angle (PCC)	0° → 94.3°	0° →119° (Zhao et al., 2016) 25° →130° (Barhoum et al., 2014) 150–153° (Atta et al., 2016)	Same trend	Different surfactants, coating dosage, crystal morphology and testing conditions.
Surface free energy (mJ/m^2)	76–78 → 38–39	Limited quantitative studies	New comparative data	Commercial GCC and PCC were systematically evaluated under the same characterization protocol.
Zeta potential (mV)	Positive → Negative (+19.6→−9.5; +12.4→−14.4)	Positive → approximately −10 (Song et al., 2003)	Good agreement	Adsorption of stearate species changes surface charge.
Bulk density	Increased after coating	Limited quantitative data	New contribution	Broader PSD and improved particle packing increase bulk density.
Moisture content	Decreased after coating	Limited quantitative data	New contribution	Hydrophobic coating suppresses water adsorption.

The results collectively demonstrate that the intrinsic particle morphology governs the response of calcium carbonate to stearic acid coating. GCC consists of relatively dense, non-porous particles, whereas PCC is composed of porous aggregates formed by nanosized primary crystals. Consequently, coating modifies not only the surface chemistry but also the packing characteristics and accessibility of internal surfaces. This explains why both materials become hydrophobic after coating while exhibiting different responses in BET surface area, pore volume, bulk density, and moisture content. The decrease

in surface free energy is directly reflected by the increase in water contact angle and the change in zeta potential, confirming successful adsorption of stearic acid onto both materials. Therefore, the observed changes in the measured properties should be interpreted as interconnected consequences of particle morphology, pore structure, and surface modification rather than as isolated phenomena.

The overall relationship between the intrinsic morphology of the materials, stearic acid adsorption, and the resulting changes in the physical and surface properties is schematically illustrated in Fig. 11. Accordingly, both Table 5 and Fig. 11 and the accompanying discussion provide an integrated interpretation of the present results in the context of previous studies.

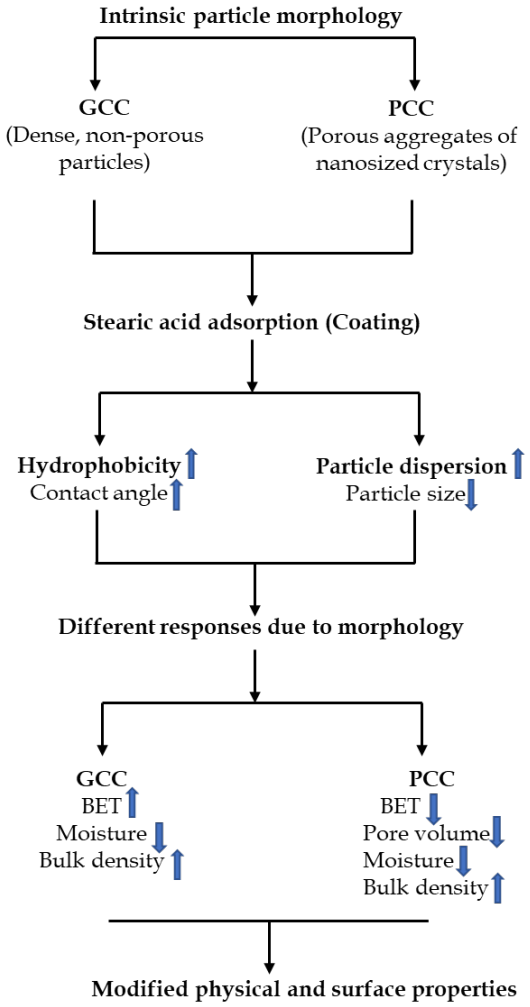

Fig. 11. Proposed mechanism illustrating the effect of stearic acid coating on the physical and surface properties of commercial GCC and PCC

4. Conclusions

The results of this study can be summarized as follows:

- The coating process broadened the PSD curves of both products (GCC and PCC) and resulted in an overall decrease in particle size. The average particle sizes were 2.59/2.03/8.49/6.82 µm for GCC/M-GCC/PCC/M-PCC, respectively. However, this decrease is more pronounced at finer particle sizes and diminishes and disappears as the size increases. This is likely because hydrophobic attractive forces become effective on relatively coarse particles, hindering potential dispersion due to reduced surface energy.
- The coating process resulted in an increase in the surface area of GCC (from 4.28 m^2/g to 5.54 m^2/g), while causing a decrease in the surface area of PCC (from 30.03 m^2/g to 19.79 m^2/g). According to SEM and mercury porosimetry analyses, this was attributed to the aggregate/particle morphology of PCC, which consists of nanosized primary crystal grains and exhibits porosity.

- According to the porosity analysis results, it was determined that the total pore volume of PCC decreased from 1.04 cm^3/g to 0.83 cm^3/g after the coating process. This behavior may be associated with partial pore filling by SA molecules and resulting reduction in accessible pore volume.
- As expected, the moisture content of both products decreased after coating, but the decrease was greater in PCC. The measured moisture content is as follows: GCC/M-GCC/PCC/M-PCC: 0.28/0.22/0.62/0.34 %.
- An increase in bulk (or free flowing) densities was observed in coated products (M-GCC and M-PCC). However, this increase is more pronounced in GCC. This increase can be attributed to broader particle size distributions and improved particle packing characteristics. The bulk densities of the products are as follows: GCC/M-GCC/PCC/M-PCC: 0.60/0.73/0.38/0.41 g/cm^3.
- GCC and PCC, which exhibit hydrophilic or superhydrophilic properties, became hydrophobic following the coating process. However, it was determined that M-GCC ($\theta_w \approx 129^o$) exhibited greater hydrophobicity than M-PCC ($\theta_w \approx 94^o$). Consistent with the θ_w data, the OWRK-Fowkes surface free energies (SFE) values for GCC, M-GCC, PCC, and M-PCC were determined to be 76, 39.2, 78.2, and 38.5 mJ/m^2, respectively. Following the coating process, the SFE values of the products decreased by approximately half.
- The positive zeta potential (ZP) observed prior to coating (GCC = 19.6 mV; PCC = 12.4 mV) shifted to a negative value after the coating process. Furthermore, it was determined that the ZP value of M-PCC (-14.4 mV) was more negative than that of M-GCC (-9.5 mV).

In conclusion, SA (stearic acid)-based hydrophobic coating products have a significant impact not only on the surface properties, such as contact angle, surface energy, and zeta potential, of natural (GCC) and synthetic (PCC) calcites, but also on their physical properties, including particle size, surface area, porosity, moisture content, and bulk density. This effect manifests at different levels depending on the GCC and PCC particle morphologies and, of course, on the companies' coating process conditions.

Acknowledgments

This study was conducted as part of the master's thesis project entitled "Comparison of the Distribution of Calcite and Modified (Steric Acid Coated) Calcite in Epoxy" (code "25.FEN.BİL.01"), financially supported by the AKU-BAPK unit. We thank the AKU-BAPK unit for their support. We also thank Adaçal Industrial Minerals Inc. for their support with the characterization studies and Nidaş Inc. for providing samples.

References

ATTA, A.M., AL-LOHEDAN, H.A., EZZAT, A.O., AL-HUSSAIN, S.A., 2016. *Characterization of superhydrophobic epoxy coatings embedded by modified calcium carbonate nanoparticles*. Prog. Org. Coat., 101, 577–586. http://dx.doi.org/10.1016/j.porgcoat.2016.10.008

BARHOUM. A., EL-SHEIKH, S.M., MORSY, F., EL-SHERBINY, S., RENIERS, F., DUFOUR, T., DELPLANCKE, M.P., VAN ASSCHE, G., RAHIER, H., 2014. *Preparation and characterization of ultra-hydrophobic calcium carbonate nanoparticles*. 2nd International Conference on Structural Nano Composites (NANOSTRUC 2014). IOP Conf. Series: Materials Science and Engineering 64 (2014) 012037 doi:10.1088/1757-899X/64/1/012037

BERNS, R.S., 2000. *Billmeyer and Saltzman's Principles of Color Technology* (3rd Edition). Wiley Interscience, p. 272, New York. (ISBN-13: 978-0471194590).

CAO, Z., DALY, M., CLÉMENCE, L., GEEVER, L.M., MAJOR, I., HIGGINBOTHAM, C.L., DEVINE, D.M., 2016. *Chemical surface modification of calcium carbonate particles with stearic acid using different treating methods*. Applied Surface Science 378, 320–329. http://dx.doi.org/10.1016/j.apsusc.2016.03.205

CROITORU, C., PASCU, A., ROATA, I.C., STANCIU, E.M., 2017. *Obtaining and characterization of polyolefin-filled calcium carbonate composites modified with stearic acid*. International Conference on Innovative Research, IOP Conference Series: Materials Science and Engineering, vol 209, 012041, doi: 10.1088/1757-899X/209/1/012041

ÇAYIRLI, S., GÖKÇEN, H.S., DAĞCI, E., 2020. *Surface Modification of Calcite With Stearic Acid Using Dry Method*. NOHU J. Eng. Sci.; 9(2): 1054-1064. https://doi.org/10.28948/ngumuh.695163

ERSOY, B., ÇIFTÇI, H., AL-SALAHI, S.A., EVCIN, A., 2026. *Comparison of some characteristic properties of natural and synthetic calcites as commercial fillers*. Engineering Perspective, 6(3), 319-330. https://doi.org/10.64808/engineeringperspective.1880759

GILL, R., SCOTT, W., 1987. *The relative effects of different calcium carbonate filler pigments on optical properties*. Tappi J. 70 (1): 93-99. https://www.semanticscholar.org/paper/The-relative-effects-of-different-calcium-carbonate-Gill-Scott/5bc226759a6c3637e22eab29ce625bf17c49e050

GHOSH, S.K., WAGHOO, G., KHANNA, A.S., RAJESH KUMAR, K., ANSARIA, F.Y., YADAV, K., SEN, A.K., 2012. *Synergistic effect of surface functionalized calcite with binder on epoxy coating performance*. Progress in Organic Coatings 75, 14–19. https://doi.org/10.1016/j.porgcoat.2012.03.001

HUANG, Y., MA, L., HUANG, Z., LAI, W. ZHENG, Y., XU, M., YANG, A., LIANG, L., LU, Z., ZHOU, J., ZHU, Y., 2025. *Effect of stearic acid and sodium stearate on hydrophobicity of nano calcium carbonate and mechanism of water vapor adsorption*. Sci Rep 15, 364. https://doi.org/10.1038/s41598-024-82802-z

KLEBA-EHRHARDT, R., JASTRAM, B., HEINZE, C., GORDEI, A., GURLO, A., KARL, D., 2025. *Effect of relative humidity on powder flowability and powder bed formation in additive manufacturing*. Additive Manufacturing, 109, 104862. https://doi.org/10.1016/j.addma.2025.104862

KROSCHWITZ, J.I., 1990. *Concise Encyclopedia of Polymer Science and Engineering*. Wiley, New York, 1990. DOI:10.5860/choice.28-3065

LAM, T.D., HOANGA, T.V., QUANGB, D.T., KIM, J.S., 2009. *Effect of nanosized and surface-modified precipitated calcium carbonate on properties of $CaCO_3$/polypropylene nanocomposites*. Materials Science and Engineering A 501, 87–93. doi:10.1016/j.msea.2008.09.060

LIN, Y., CHEN, H., CHAN, C.M., WUB, J., 2011. *Effects of coating amount and particle concentration on the impact toughness of polypropylene/$CaCO_3$ nanocomposites*. European Polymer Journal 47, 294–304. https://doi.org/10.1016/j.eurpolymj.2010.12.004

LIN, R.Y., ZHANG, J.Y., & ZHANG, P.X., 2002. *Nucleation and growth kinetics in synthesizing nanometer calcite*. Journal of Crystal Growth, 245(3–4), 309–320. https://doi.org/10.1016/S0022-0248(02)01739-6

LU, S., PUGH, R.J., FORSSBERG, E., 2005. *Interfacial Separation of Particles*. Elsevier, Amsterdam, p. 694. https://doi.org/10.1016/S1672-2515(07)60272-3

MIHAJLOVIĆ, S.R., VUČINIĆ, D.R., SEKULIĆ, Z.T., MILIĆEVIĆ, S.Z., KOLONJA, B.Z., 2013. *Mechanism of stearic acid adsorption to calcite*. Powder Technology, 245, 208–216. http://dx.doi.org/10.1016/j.powtec.2013.04.041

NAYDOWSKI, C., HESS, P., STRAUCH, D., KUHLMANN, R., ROHLEDER, J., 2001. *Calcium Carbonate and Its Industrial Application in Calcium Carbonate: From the Cretaceous Periolt into the 21st Century*. Ed: Tegethoff FW, Birkhauser Verlag, p342, Berlin. https://doi.org/10.1007/978-3-0348-8245-3

PAL, A., SEVONKAEV, I., BARTLING, B., RIJSSENBEEK, J., GOI, D.V., 2014. *Dipentaerythritol: A novel additive for the precipitation of dispersed Ni particles in polyols*. RSC Adv., 4, 20909-20914. DOI: 10.1039/c4ra01464b

REED, J.S., 1994. *Principles of Ceramics Processing (second edition)*. John Wiley & Sons Inc., 658p, New York.

RODRIGUEZ-BLANCO, J.D., SHAW, S., BENNING, L.G., 2011. *The kinetics and mechanisms of amorphous calcium carbonate (ACC) crystallization to calcite, via vaterite*. Nanoscale, 3, 265, DOI: 10.1039/c0nr00589d

ROHLEDER, J., HUWALD, E., 2001. *Calcium Carbonate and Its Industrial Application in Calcium Carbonate: From the Cretaceous Periolt into the 21st Century*. Ed: Tegethoff FW, Birkhauser Verlag, p342, Berlin. https://doi.org/10.1007/978-3-0348-8245-3

SAÇAK, M., 2005. *Polymer Technology* (in Turkish). Gazi Bookstore, p. 461, Ankara. ISBN: 9786053445258

SALISBURY, J.W., WALTER, L.S., VERGO, N., D'ARIA, D.M., 1991. *Infrared (2,1-25 μm) Spectra of Minerals*. The John Hopkins University Press, 267p, Baltimore.

SHANEFIELD, D.J., 1996. *Organic Additives and Ceramic Processing (second edition)*. Kluwer Academic Publishers, 311p, Boston.

SHI, X., ROSA, R., LAZZERI, A., 2010. *On the coating of precipitated calcium carbonate with stearic acid in aqueous medium*. Langmuir, DOI: 10.1021/la904914h.

SHINOHARA, K., TAKAHASHI, H., 2006. *Blockage of Storage Vessels, in: Powder Technology Handbook (Third Edition)*. Eds: H. Masuda, K. Higashitani, H. Yoshida, CRC Press Taylor&Francis Group, New York.

SONG, M.G., KIM, J.Y., KIM, J.D., 2003. *Effect of sodium stearate and calcium ion on dispersion properties of precipitated calcium carbonate suspensions*. Colloids and Surfaces A: Physicochem. Eng. Aspects 229, 75–83. doi:10.1016/j.colsurfa.2003.08.016

SUZUKI, M., 2006. *Packing Properties*. In H. Masuda, K. Higashitani, & H. Yoshida (Eds.), Powder technology handbook (3rd ed., pp. 293–307). CRC Press. https://doi.org/10.1201/9781439831885-29

STUART, B., GEORGE, W.O., MCINTYRE, P.S., 1998. *Modern Infrared Spectroscopy*. Ando DJ(Ed), John Wiley & Sons, 176p, New York.

TEYCHENÉ, S., RODRÍGUEZ-RUIZ, I., & RAMAMOORTHY, R.K., 2020. *Reactive crystallization: From mixing to control of kinetics by additives*. Current Opinion in Colloid & Interface Science, 46, 1–19. https://doi.org/10.1016/j.cocis.2020.01.003

UÇURUM, M., ÖZDEMIR, A., 2024. *Wet mechanochemical surface modification of calcite employing an integration of conventional design and analytical hierarchy process*. Powder Technology 443, 119970. https://doi.org/10.1016/j.powtec.2024.119970

ULUSOY, U., 2023. *A review of particle shape effects on material properties for various engineering applications: from macro to nanoscale*. Minerals, 13, 91. https://doi.org/10.3390/min13010091

WYPYCH, G., 2000. *Handbook of Fillers (2nd Edition)*. ChemTec Publishing, Toronto. ISBN 1-895198-19-4.

YILDIZ, A., GENÇ, Ö., BEKTAŞ, S., 1997. *Instrumental Analysis Methods (second edition)* (in Turkish), Hacettepe University Press, p. 506, Ankara. ISBN: 9789754910285

ZHANG, Z., LIU, X., BAN, X., JI, J., TIAN, P., YANG, Y., 2025. *The influence of filler types and content on the curing behavior and properties of a bio-based polyurethane engineered sealant*. International Journal of Adhesion & Adhesives 136, 103866. https://doi.org/10.1016/j.ijadhadh.2024.103866

ZHAO, L., ZHANG, Y., MIAO, Y., NIE, L., 2016. *Controlled synthesis, characterization and application of hydrophobic calcium carbonate nanoparticles in PVC*. Powder Technology 288, 184–190, http://dx.doi.org/10.1016/j.powtec.2015.11.001

ZHANG, H., ZHOU, X., GUO, H., ZHANG, Y., LI, D., YE, F., TONG, Y., WANG, Z., 2024. *Effects of particle size and modifier amount on hydrophobicity of as-synthesized and modified nano-silica spheres*. Ceramics International 50, 21511–21518. https://doi.org/10.1016/j.ceramint.2024.03.264